Proton Conductivity and Humidity-Sensing Properties at High Temperature of the NASICON-Based Composite Material $HZr_2P_3O_{12}$·ZrP_2O_7

Shouhua Feng† and Martha Greenblatt*

Department of Chemistry, Rutgers, The State University of New Jersey, Piscataway, New Jersey 08854-0939

Received June 5, 1992. Revised Manuscript Received July 7, 1993®

Proton conductivity and humidity-sensing characteristics of a composite material, $HZr_2P_3O_{12}$·ZrP_2O_7, were investigated by an ac impedance technique in the temperature range 350–600 °C in dry He, moist He, H_2, and O_2 atmosphere, respectively. The conductivity of $HZr_2P_3O_{12}$·ZrP_2O_7 increases linearly with increasing relative humidity or hydrogen gas concentration at ~450 °C. The increase of conductivity of $HZr_2P_3O_{12}$·ZrP_2O_7 with increasing water vapor or hydrogen gas pressure is consistent with the reaction $H_2O(gas) \rightarrow H^+ + {}^1/_2O_2 + 2e^-$ occurring at the electrode–electrolyte interface. The real part of the complex impedance as a function of relative humidity or H_2 gas pressure is independent of frequency in the range 10–20 Hz. These results indicate that the $HZr_2P_3O_{12}$·ZrP_2O_7 composite ceramic is applicable for humidity and H_2 gas sensing.

Introduction

The enhancement of proton conduction upon increase of water vapor pressure is found in many conductive materials. Some of these materials exhibit proton conductivity due to water adsorption on the surface, where protonation occurs through ionization of sorbed water and surface hydroxyl groups.[1] For this type of material, the proton conductivity is limited up to temperatures where the water is retained in the material (i.e., this type of water is usually lost below 200 °C). Some materials, however, show protonic and/or electronic conductivity at high temperature (200–1000 °C) in the presence of water vapor, while at relatively low temperature they are not conductive. In the latter case, protonation and protonic conduction is induced by the reaction of water molecules at the interface of the electrolyte–electrode[2] or by H_2O–hole interaction.[3] These characteristics have given rise to the development of conductimetric type humidity-sensing materials.[4–10]

Most of the humidity-sensing materials used at high temperature are based on sintered metal oxides, including $SrCeO_3$-based electrolytes,[3] $MgCrO_4$–TiO_2,[4–6] ZrO_2–MgO,[6] $Ba_{0.5}Sr_{0.5}TiO_3$,[7] (Pb,La)(Zr,Ti)O_3,[8] TiO_2–$K_2Ti_6O_{13}$,[9] and rutile-phase TiO_2.[10] These materials are sensitive to humidity and/or have multifunctional sensing characteristics (humidity–gas or humidity–temperature). At high temperature, they exhibit ionic conductivity or semiconductor behavior. Recently we reported on the sintered composite ceramic $HZr_2P_3O_{12}$·ZrP_2O_7, which exhibits excellent humidity-sensing properties at high temperatures as a solid electrolyte in a galvanic cell humidity sensor.[11] The major phase of this electrolyte, $HZr_2P_3O_{12}$, in contrast to the materials mentioned above contains protons. $HZr_2P_3O_{12}$ has a three-dimensional NASICON-type framework structure with interconnected channels for ionic motion. The structural properties of $HZr_2P_3O_{12}$ are consistent with bulk proton conduction without hole or electronic charge transport. Further, the galvanic cell investigations,[11] particularly the results of a H_2 concentration cell employing the $HZr_2P_3O_{12}$·ZrP_2O_7 composite, which showed the transference number to be close to unity, provided strong evidence for proton conductivity in this material.

In this paper we present results of complex impedance studies on the proton conductivity and the conductimetric humidity sensing properties of the $HZr_2P_3O_{12}$-based material at tempertures above 400 °C.

Experimental Section

$HZr_2P_3O_{12}$ was prepared by heating $(NH_4)Zr_2P_3O_{12}$ in air at 650 °C for 5 h. $(NH_4)Zr_2P_3O_{12}$ was synthesized by a hydrothermal method in a stainless steel autoclave lined with polytetrafluoroethylene (PTFE) from an aqueous mixture of $ZrOCl_2$·$8H_2O$ (Aldrich Chem. Co., Inc.) and $(NH_4)H_2PO_4$ (Fisher Scientific) according to a method described previously.[12] α-ZrP ($Zr(HPO_4)_2$·H_2O) was synthesized according to an established procedure.[13] The NASICON-based material examined in this work was the sintered composite ceramic composed of $HZr_2P_3O_{12}$·ZrP_2O_7. The sample preparation was the same as in a previous study.[11] The sintered sample was analyzed by powder

† Present address: Department of Chemistry, Jilin University, Changchun, China.

* To whom correspondence should be addressed.

® Abstract published in *Advance ACS Abstracts*, August 15, 1993.

(1) Anderson, J. H.; Parks, G. A. *J. Phys. Chem.* **1968**, *72*, 3662.
(2) Raistrick, I. D. *Impedance Spectroscopy*; Macdonald, J. R., Ed.; John Wiley & Sons: New York, 1987; p 64.
(3) Uchida, H.; Maeda, N.; Iwahara, H. *Solid State Ionics* **1983**, *11*, 117.
(4) Nitta, T.; Terada, Z.; Hayakawa, S. *J. Am. Ceram. Soc.* **1980**, *63*, 295.
(5) Nitta, T.; Terada, Z.; Fukushima, F. *IEEE Trans. Electron Devices* **1982**, *ED-29*, 95.
(6) Nitta, T.; *Chemical Sensor Technology*, Seiyama, T., Ed.; Elsevier: Tokyo, 1988; Vol. 1, p 57.
(7) Yeh, Y. C.; Tseng, T. Y. *J. Mater. Sci. Lett.* **1988**, *7*, 766.
(8) Sadaoka, Y.; Matsuguchi, M.; Sakai, Y.; Aono, H.; Nakayama, S.; Kuroshima, H. *J. Mater. Sci.* **1987**, *22*, 3685.
(9) Yeh, Y. C.; Tseng, T. Y.; Chang, D. A. *J. Am. Ceram. Soc.* **1990**, *73*, 1992.
(10) Yeh, Y. C.; Tseng, T. Y.; Chang, D. A. *J. Am. Ceram. Soc.* **1989**, *72*, 1473.
(11) Feng, S.; Greenblatt, M. *Chem. Mater.* **1992**, *4*, 1257.
(12) Clearfield, A.; Roberts, B. D.; Subramanian, M. A. *Mater. Res. Bull.* **1984**, *19*, 219.
(13) Alberti, G.; Torracca, E. *J. Inorg. Nucl. Chem.* **1968**, *30*, 317.

0897-4756/93/2805-1277$04.00/0

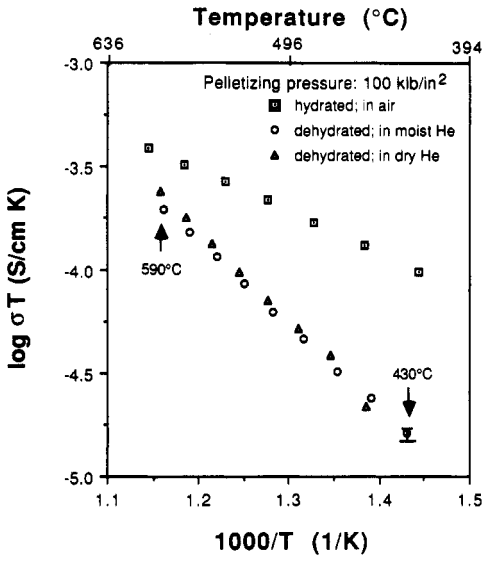

Figure 1. Arrhenius plots of conductivity of hydrated and dehydrated $HZr_2P_3O_{12}$ with pelletizing pressure 100 klb/in^2 in air, moist He, and dry He.

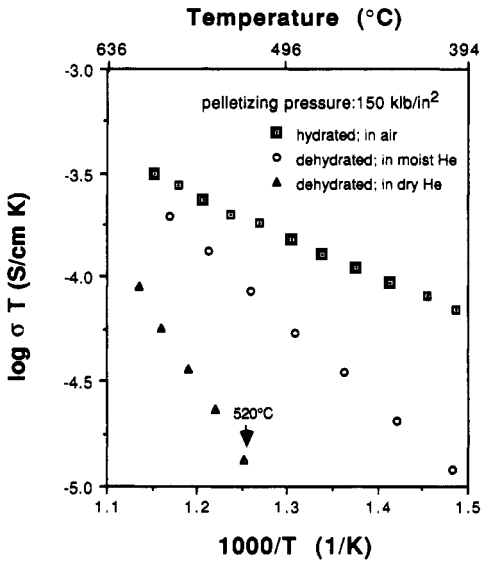

Figure 2. Arrhenius plots of proton conductivity of the hydrated and dehydrated $HZr_2P_3O_{12}$ with pelletizing pressure 150 klb/in^2 in air, moist He, and dry He.

X-ray diffraction (XRD) to ascertain the formation of the two single phases in the composite (i.e., $HZr_2P_3O_{12}$ and ZrP_2O_7).

Ionic conductivities were measured by an ac impedance technique using a Solartron Model 1250 frequency analyzer and 1186 electrochemical interface that were equipped with a Hewlett Packard 9816 desktop computer for data collection and analysis. Electrode connection to the samples were made by coating the faces of the pellets with porous platinum. A frequency range 10 Hz to 65 kHz and a heating rate of 2 °C/min were used throughout. The pelletizing pressures used were 100 and 150 klb/in^2.

To reduce the influence of the initial content of water in the sample (i.e., due to adsorption), the samples used for ac impedance measurement were first preheated to 600 °C and then cooled to 300 °C in flowing He, prior to collecting impedance data, except for the hydrated $HZr_2P_3O_{12}$ samples. The humidity in He gas was controlled by adjusting the ratio of the flow rate of the He gas saturated with water vapor to the flow rate of dry He gas at any given temperature. In one experiment, oxygen gas saturated with water vapor was used to examine the effect of O_2 gas on the conductivity. For the measurements of conductivity in H_2 environment mixed H_2–He gases with different H_2 concentrations in volume were used.

Thermogravimetric analysis (TGA) was carried out with a du Pont Model 9900 thermal analyzer using a heating rate of 10 °C/min.

Results and Discussion

Proton Conductivity of $HZr_2P_3O_{12}$ in Moist and Dry He. Figure 1 shows Arrhenius plots of conductivity in air and in moist (moist He in the figures and discussion corresponds to 100% relative humidity (RH) at 25 °C) and dry He, respectively, of an as-prepared $HZr_2P_3O_{12}$ sample, which was pelletized under 100 klb/in^2 pressure. The density of pellets prepared at 100 klb/in^2 is ~75% of the ideal. The as-prepared sample is a hydrate, $HZr_2P_3O_{12}\cdot 0.5H_2O$ (determined by TGA), and it exhibits a higher conductivity and lower activation energy than the dehydrated sample. The dehydrated sample was obtained by heating the hydrated sample $HZr_2P_3O_{12}\cdot 0.5H_2O$ to >600 °C in air. The higher conductivity of the hydrated sample is attributed to the association of water molecules with the mobile protons in the channels of the NASICON structure. For the dehydrated sample, the diffusion of protons must occur via hopping between adjacent cation lattice sites; this process leads to the high activation energy observed. Although the conductivity of the hydrated sample is higher than that of the dehydrated sample, the conductivity of the dehydrated sample is not affected by moisture in the atmosphere; i.e., the conductivity of the dehydrated sample is the same in both moist and dry He as shown in Figure 1. These results indicate that the conductivity of the $HZr_2P_3O_{12}$ sample at a pelletizing pressure of 100 klb/in^2 is sensitive to the initial water content in the lattice but not to changes in humidity. It seems that the external water introduced (i.e., moist He flow) is not adsorbed by the $HZr_2P_3O_{12}$ sample in this temperature range (450–600 °C).

Figure 2 shows Arrhenius plots of the conductivity of a hydrated $HZr_2P_3O_{12}\cdot 0.5H_2O$ pellet in air and a dehydrated $HZr_2P_3O_{12}$ pellet in moist and dry He, respectively; the sample pellets in Figure 2 were prepared with a pelletizing pressure of 150 klb/in^2. The density of these pellets is ~90% of the ideal. The conductivity of the hydrated sample does not seem to be affected by the higher pelletizing pressure (Figure 1). However, in contrast to Figure 1, the conductivity of the dehydrated sample is dramatically different in dry and moist He (Figure 2).

Comparison of the two samples prepared at different pelletizing pressure (Figures 1 and 2) suggests that a higher pelletizing pressure increases moisture sensitivity. This improvement of the sensitivity to humidity may be due to changes in the structure of the grain boundary region and/or surface at the electrode–electrolyte interface by the higher pelletizing pressure.

Proton Conductivity of $HZr_2P_3O_{12}\cdot ZrP_2O_7$ Composite. To achieve proton conductivity below 520 °C (the conductivity of dehydrated $HZr_2P_3O_{12}$ is negligibly small below ~520 °C; Figure 2) and to obtain a dense pellet sample (i.e., pure $HZr_2P_3O_{12}$ powder could not be sintered into a dense pellet), we prepared a composite, $HZr_2P_3O_{12}\cdot ZrP_2O_7$, which we also used as a humidity sensing electrolyte in a galvanic cell.[11] The initial motivation to use the composite was to achieve a dense pellet required for the galvanic cell type humidity sensing application. Subsequently, we found that the addition of an ionically insulating compound, ZrP_2O_7, increased the humidity sensitivity of $HZr_2P_3O_{12}$.

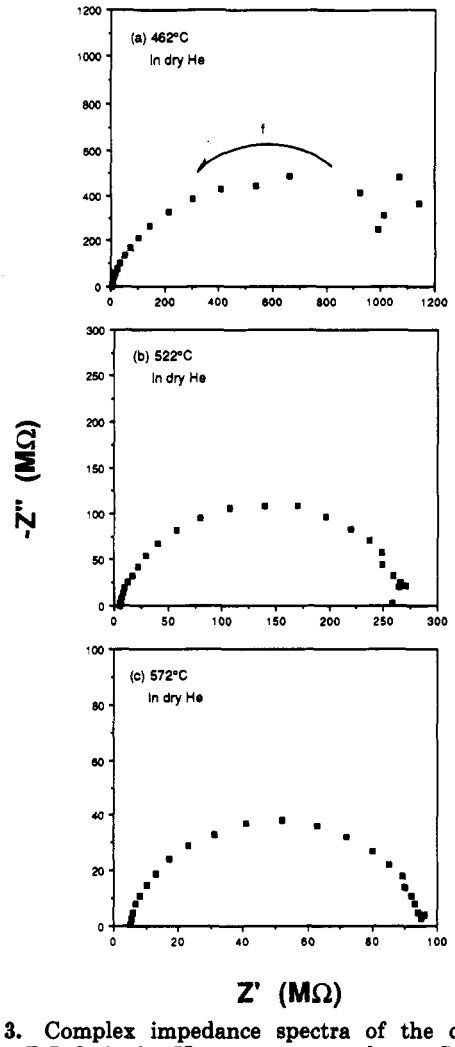

Figure 3. Complex impedance spectra of the composite $HZr_2P_3O_{12}$·ZrP_2O_7 in dry He at 462, 522, and 572 °C.

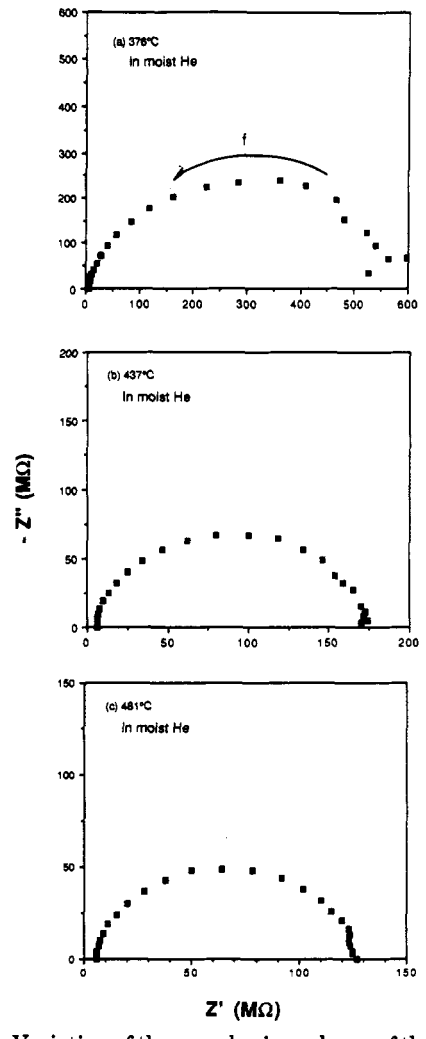

Figure 4. Variation of the complex impedance of the composite $HZr_2P_3O_{12}$·ZrP_2O_7 in moist He at 376, 437, and 481 °C.

The impedance plots of the $HZr_2P_3O_{12}$·ZrP_2O_7 composite at (a) 462, (b) 522, and (c) 572 °C in dry He are shown in Figure 3. The range of frequencies used in the measurement was limited to 10 Hz to 65 kHz by the experimental equipment. In this frequency range, a single semicircular arc is observed in each of the impedance plots. In general, this behavior is unlike that in many polycrystalline materials, where two arcs, usually representing intragrain and intergrain impedances, are seen. The observation of a single semicircle is attributed to bulk conductivity due to the high density of the sample (~85% of the ideal). The magnitude of capacitance (e.g., $C \sim 10^{-14}$ farads in Figure 6 for RH = 0) obtained from the Cole–Cole plots is consistent with bulk conductivity. Figure 4 shows the impedance plots of the $HZr_2P_3O_{12}$·ZrP_2O_7 composite at (a) 376, (b) 437, and (c) 481 °C in moisture. It is noteworthy that in the presence of water vapor the conductivity is significant below 450 °C, while under dry conditions, the conductivity is negligible below 450 °C (Figure 2).

The Arrhenius plots of conductivity of the NASICON-based composite in dry and moist He gas respectively are shown in Figure 5. Even in dry conditions the composite sample exhibits relatively high conductivity above 450 °C. The conductivity (σ) in moist conditions is higher and the activation energy (E_a) is lower than in dry conditions. The observed higher E_a and lower σ in dry conditions is attributed to the lower concentration of H^+ and the lack of sufficient water molecules to facilitate proton motion in the NASICON channels of the $HZr_2P_3O_{12}$ conducting phase of the composite.

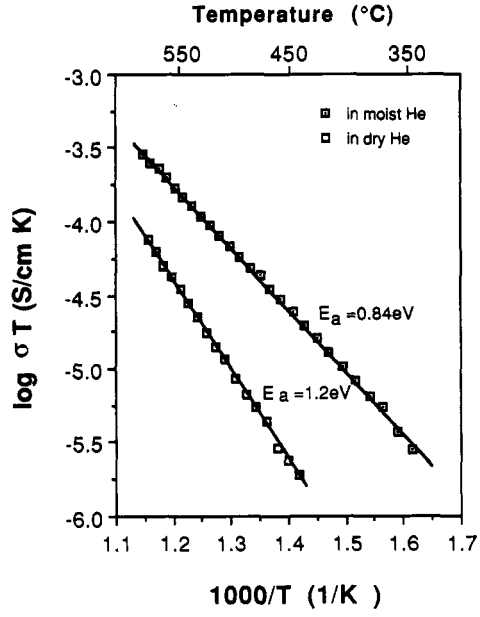

Figure 5. Arrhenius plots of proton conductivity of the NASICON-based material $HZr_2P_3O_{12}$·ZrP_2O_7 in dry and moist He.

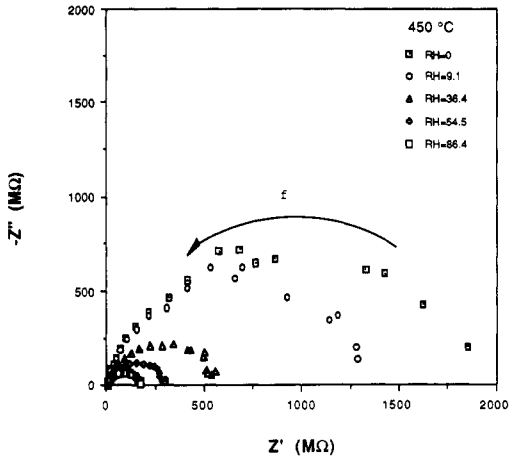

Figure 6. Variation of the complex impedance for the composite $HZr_2P_3O_{12}\cdot ZrP_2O_7$ as a function of humidity at 450 °C.

It appears that proton motion in the $HZr_2P_3O_{12}\cdot ZrP_2O_7$ composite occurs at ~450 °C and the dramatic increase of the conductivity in moist conditions at ~450 °C (Figure 5) must be attributed to the contribution of protons from the external water vapor. On the basis of our galvanic cell studies and dc measurement of conductivity on $HZr_2P_3O_{12}\cdot ZrP_2O_7$ pellets, as well as the results reported here, 450 °C is the optimal temperature of sensitivity for humidity sensing in this material.[11]

Humidity Sensing Properties. In Figure 6, the variation of complex impedance with relative humidity at 450 °C indicates that the resistance of the sample decreases dramatically with increasing relative humidity. Similar to the impedance behavior of the sample in dry He, only one semicircle is observed in the impedance spectrum with a change of humidity, but the center of each arc is displaced below the real axis, which implies possible reactions at the electrode–electrolyte interface.

Figure 7 shows the humidity dependence of the conductivity of the $HZr_2P_3O_{12}\cdot ZrP_2O_7$ composite at 450, 500, and 550 °C, respectively. The conductivity increases with increasing humidity in the whole range of temperature examined and the plot of conductivity vs humidity is nearly linear except for the region of low humidity (RH < 20%) in each case.

The variation of Z' vs log frequency, f, at 450 °C in Figure 8 shows that the real part of impedance as a function of humidity is frequency independent in the low-frequency region (10–20 Hz). This is advantageous for device application, because it requires the use of a single low-frequency for the measurements of impedance for humidity sensing.

Proposed Mechanism of Proton Conduction. Strong evidence of proton transport in this material was provided by the emf measurmeents in a galvanic cell: (a) The transference number was close to unity in a hydrogen concentration cell. (b) In a steam concentration cell, the emf was proportional to the water vapor pressure of the sample gas (P_{H_2O}) according to the Nernst equation, $E = RT/2F \ln P_{H_2O}(P_{O_2}^{ref})^{1/2}/P_{H_2O}^{ref}(P_{O_2})^{1/2}$ ($P_{O_2}^{ref} = P_{O_2}$ in atmospheric conditions); this behavior is consistent with the proposed redox reactions: $H_2O \rightarrow 2H^+ + {}^1/_2O_2 + 2e^-$ at the anode and $2H^+ + {}^1/_2O_2 + 2e^- \rightarrow H_2O$ at the cathode. (c) The emf was proportional to the oxygen pressure according to the Nernst equation in a wet O_2 concentration cell, which is further evidence for the redox reactions, cited above, occurring at the electrodes, and proton transport through the electrolyte.[11]

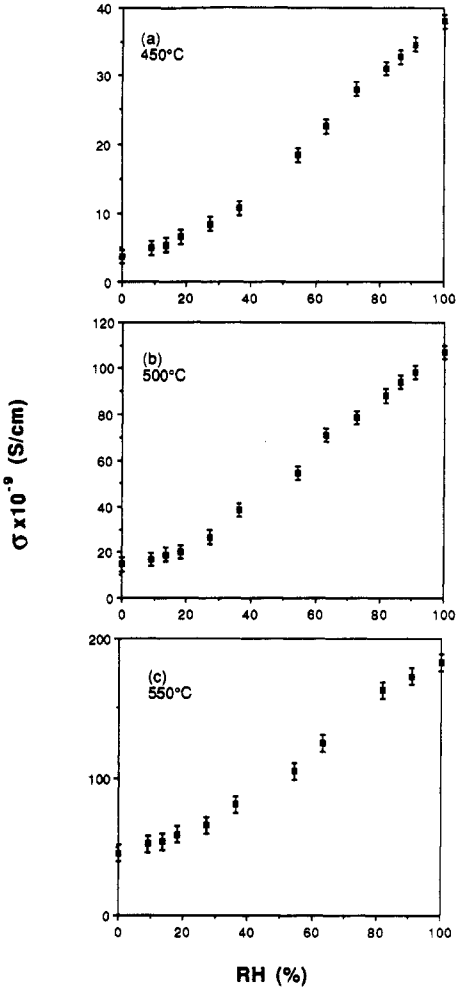

Figure 7. Humidity dependence of conductivity of the $HZr_2P_3O_{12}\cdot ZrP_2O_7$ determined from ac impedance measurements at 450, 500, and 550 °C.

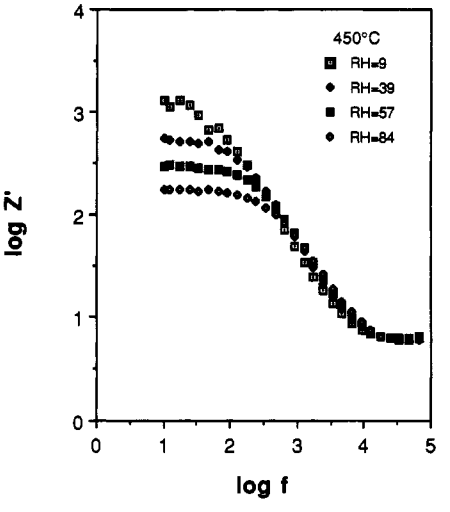

Figure 8. Frequency dependence of impedance of the $HZr_2P_3O_{12}\cdot ZrP_2O_7$ composite in moist He at 450 °C.

Here we continue to investigate the mechanism of proton conductivity in this material based on the impedance results.

As we mentioned above, at 450 °C, the conductivity of the composite $HZr_2P_3O_{12}\cdot ZrP_2O_7$ sample in moisture is

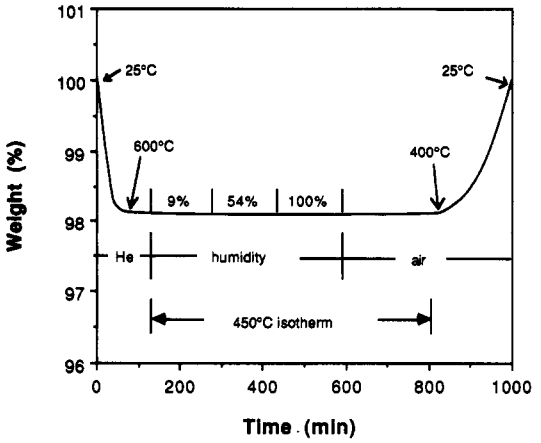

Figure 9. TGA curve of $HZr_2P_3O_{12}{\cdot}ZrP_2O_7$ under various conditions.

about 1.5 orders of magnitude higher than that in dry He. There are two possible reasons for the enhancement of conductivity by water vapor at high temperatures. One is due to the chemisorption of water on the grain or pore surfaces of the ceramic sample. The adsorbed water molecules or surface hydroxyl groups formed by water chemisorption release protons into the sample as follows:

$$H_2O(\text{surface}) = H^+(\text{bulk}) + OH^-(\text{surface}) \quad (1)$$

The proton conductivity is expected to increase with the increase of the mobile proton concentration which is proportional to the content of adsorbed water on the surface of the sample. Another possible mechanism for the increase of proton conductivity with increasing P_{H_2O} may be due to a charge transfer reaction at the electrode–sample interface. In this case, the reaction at the interface is

$$H_2O(\text{gas}) = 2H^+(\text{electrolyte}) + {}^1/_2O_2 + 2e^-(\text{electrode}) \quad (2)$$

The formation of proton by this reaction could be responsible for the increase of proton conductivity of the sample. Equation 2 is also consistent with the mechanism of protonation proposed in the galvanic cell.[11]

It is obvious that the adsorption of water on the grain or pore surface of the sample is critical for reaction 1. For reaction 2, the adsorption of water could be restricted only to the electrode–electrolyte interface.

To clarify the mechanism of protonation in this material, two experiments TGA measurements in various atmospheres and ac impedance measurements in hydrogen, were carried out. Figure 9 shows the TGA results for various conditions. A disk-shaped sample used for the ac impedance analysis was employed. In an evacuated TGA chamber, the sample was first heated to 600 °C in a He flow. A total weight loss of 1.9% was observed, corresponding to an initial formula of $HZr_2P_3O_{12}{\cdot}ZrP_2O_7{\cdot}0.4H_2O$. The sample was then cooled in a flow of He to 450 °C at a cooling rate of 4 °C/min. No weight gain was observed in the cooling cycle (Figure 9). An isothermal condition was maintained at 450 °C, and moist He gas with 9%, 54%, or 100% relative humidity (25 °C) was introduced into the chamber each for a period of 150 min. In 16 h a total weight change of 0.1% was observed, which is within the experimental error. This result is strong evidence that water is not significantly adsorbed on the surface of the sample at 450 °C and that reaction 1 is not the mechanism

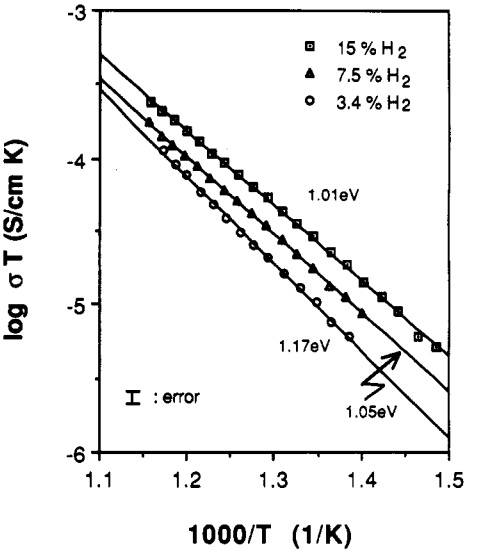

Figure 10. Temperature dependence of conductivity of $HZr_2P_3O_{12}{\cdot}ZrP_2O_7$ at hydrogen concentration of 3.4, 7.0, and 15% by volume.

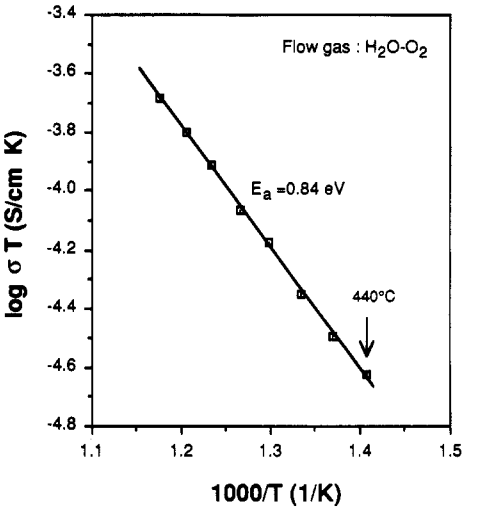

Figure 11. Effect of O_2 gas pressure on the conductivity of $HZr_2P_3O_{12}{\cdot}ZrP_2O_7$ in moist condition.

of protonation. This finding indicates that this material is a true humidity sensor. Air was then introduced and the system was allowed to equilibrate for 4 h at which time the sample was allowed to cool. During this period all the weight that had been lost was recovered.

Additional evidence in support of the mechanism given by eq 2 is provided by the ac conductivity measurements of $HZr_2P_3O_{12}{\cdot}ZrP_2O_7$ in H_2 atmosphere shown in Figure 10. The conductivity of the sample in H_2 (He as carrier gas) is higher than that in dry He (see Figure 1) and the conductivity increases with increasing H_2 gas pressure. These results support the charge-transfer reaction:

$$H_2(\text{gas}) = 2H^+(\text{electrolyte}) + 2e^-(\text{electrode}) \quad (3)$$

The effect of O_2 gas on the conductivity of $HZr_2P_3O_{12}{\cdot}ZrP_2O_7$ in moisture was also examined. The conductivity of the sample in O_2/H_2O gas below ~440 °C is insignificantly low as shown in Figure 11. Above ~440 °C, the values of conductivity and activation energy are the same as those observed in moist conditions without O_2 (Figure 5). According to eq 2, increasing of O_2 gas pressure should suppress the reaction at the electrode–electrolyte interface. However, if the reaction represented by eq 2 is

not at equilibrium, if eq 2 is irreversible, then the conductivity will not be affected by the O_2 pressure.

These results may also explain why the optimal operation temperature in the EMF-type sensor with $HZr_2P_3O_{12}$·ZrP_2O_7 electrolyte is at ~450 °C.[11] Above 450 °C, the material itself has intrinsic proton conductivity (i.e., the motion of H^+ ions in the channels of the NASICON structure), which contributes to the value of EMF. At and above 450 °C protonation occurs primarily via a mechanism described by eq 2. In contrast, below 450 °C, proton conductivity increases with increasing water vapor pressure, both because of the adsorption of water on the surface according to eq 1 (see Figure 9) and the reaction at the electrode–electrolyte interface as given by eq 2.

Conclusions

In summary, conductivity of the NASICON-based composite $HZr_2P_3O_{12}$·ZrP_2O_7 observed in dry He, moist He, and H_2 gas in the temperature range 350–600 °C is attributed to proton conductivity in the sample. In the temperature range studied, the proton conductivity of the material at a relative humidity of 100% (25 °C) and H_2 gas concentration of 15% in volume is about 1.5 orders of magnitude higher than that in dry He. The proton conductivity of the material as a function of relative humidity was found to be nearly linear at 450, 500, and 550 °C, respectively. On the basis of the experimental evidence, the protonation mechanism is via a charge-transfer reaction at the electrode–electrolyte interface according to the reaction H_2O (gas) → $2H^+$ (electrolyte) + $^1/_2O_2$ + $2e^-$. The variation of the real part of the impedance (Z') with humidity) is independent of the frequency in the range 10–20 Hz, which is advantageous for humidity-sensing device application of this composite ceramic material.

Acknowledgment. We thank Prof. W. H. McCarroll for his suggestions on improving this paper. This is publication No. D10552-7-91 of the New Jersey Agricultural Experiment Station supported by State Funds and the Center for Advanced Food Technology (CAFT). The Center for Advanced Food Technology is a New Jersey Commission on Science and Technology Center.